

2  
Conf. 880928--6

UCRL-JC--106493

DE91 011207

INTRODUCTION TO THE PHYSICS  
OF ICF CAPSULES

John D. Lindl

This paper was prepared for submittal  
to International School of Plasma Physics  
Inertial Confinement Fusion Course and  
Workshop, Varenna, Italy, Sep 6-16, 1988.

March 13, 1989

This is a preprint of a paper intended for publication in a journal or proceedings. Since changes may be made before publication, this preprint is made available with the understanding that it will not be cited or reproduced without the permission of the author.

Lawrence  
Livermore  
National  
Laboratory

MASTER

DISTRIBUTION OF THIS DOCUMENT IS UNLIMITED

*[Signature]*

#### **DISCLAIMER**

This document was prepared as an account of work sponsored by an agency of the United States Government. Neither the United States Government nor the University of California nor any of their employees, makes any warranty, express or implied, or assumes any legal liability or responsibility for the accuracy, completeness, or usefulness of any information, apparatus, product, or process disclosed, or represents that its use would not infringe privately owned rights. Reference herein to any specific commercial products, process, or service by trade name, trademark, manufacturer, or otherwise, does not necessarily constitute or imply its endorsement, recommendation, or favoring by the United States Government or the University of California. The views and opinions of authors expressed herein do not necessarily state or reflect those of the United States Government or the University of California, and shall not be used for advertising or product endorsement purposes.

INTRODUCTION TO THE PHYSICS  
OF ICF CAPSULES\*

John D. Lindl

Lawrence Livermore National Laboratory  
P. O. Box 808, L-477  
Livermore, California 94550 USA

Inertial Confinement Fusion is an approach to fusion which relies on the inertia of the fuel mass to provide confinement. To achieve conditions under which this confinement is sufficient for efficient thermonuclear burn, high gain ICF targets designed to be imploded directly by laser light have features similar to those shown in Fig. 1. These capsules are generally a spherical shell which is filled

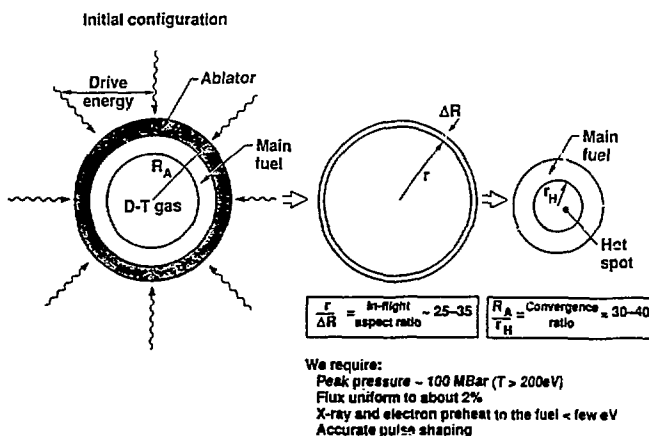


Figure 1. Features of high gain ICF targets.

\*This work performed under the auspices of the U.S. Department of Energy by the Lawrence Livermore National Laboratory under contract number W-7405-ENG-48.

with low density DT gas. The shell is composed of an outer region which forms the ablator and an inner region of frozen or liquid DT which forms the main fuel. Energy from the driver is delivered to the ablator which heats up and expands. As the ablator expands and blows outward, the rest of the shell is forced inward to conserve momentum. In this implosion process, several features are important. We define the in-flight-aspect-ratio (IFAR) as the ratio of the shell radius  $R$  as it implodes to its thickness  $\Delta R$ . Hydrodynamic instabilities during the implosion impose limits on this ratio which results in a minimum pressure requirement of about 100 Mbar. The convergence ratio is defined as the ratio of the initial outer radius of the ablator to the final compressed radius of the hot spot. This hot spot is the central region of the compressed fuel which is required to ignite the main fuel in high gain designs. Typical convergence ratios are 30-40. To maintain a nearly spherical shape during the implosion, when convergence ratios are this large, the flux delivered to the capsule must be uniform to a few percent.

To understand what conditions are required in the imploded fuel to achieve efficient thermonuclear burn, it is useful to develop a simple model for the burn of DT. The number of reactions  $n$  per second is given by:

$$\frac{dn}{dt} = N_D N_T \langle\sigma v\rangle$$

where  $\langle\sigma v\rangle$  is the reaction cross section averaged over a Maxwellian distribution of particles and

$$N_D = N_T = \frac{1}{2} N_0 - n$$

where  $N_0$  is the initial total number density. If we define the burn fraction by

$$\phi = \frac{2n}{N_0}$$

then we have:

$$\frac{d\phi}{dt} = N_0 \left(1 - \frac{\phi}{2}\right)^2 \langle\sigma v\rangle$$

If we assume that the Maxwell averaged cross section is nearly constant over the burn duration, then we can integrate this equation to obtain:

$$\frac{\phi}{1 - \phi} = \frac{N_0 \tau}{2} \langle \sigma v \rangle$$

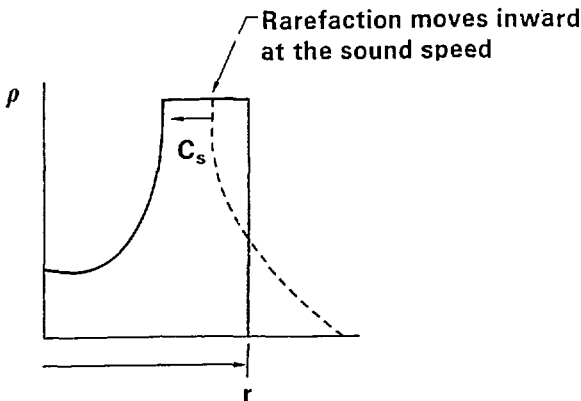
where  $\tau$  is the confinement time. In inertial confinement, burn is quenched by hydrodynamic expansion as shown in Fig. 2. From the outside of the fuel, a rarefaction moves inward at the speed of sound  $C_s$ . By the time this rarefaction has moved a fraction of the radius  $r$ , the fuel density in most of the fuel mass has dropped significantly and the fuel no longer burns efficiently. The confinement time is approximately given by:

$$\tau \sim \frac{r}{3C_s}$$

Hence, we can write the burn efficiency as:

$$\frac{\phi}{1 - \phi} = \frac{N_0 \langle \sigma v \rangle}{6} \frac{r}{C_s}$$

The cross section for DT and several other thermonuclear fuels is shown in Fig. 3. For DT between 20 and 40 KeV, which is typical of the burn of ICF capsules, the ratio of the cross section to the sound speed is



$$\text{Confinement time } \tau \sim \frac{r}{3C_s}$$

Figure 2. In inertial confinement fusion, burn is quenched by hydrodynamic expansion.

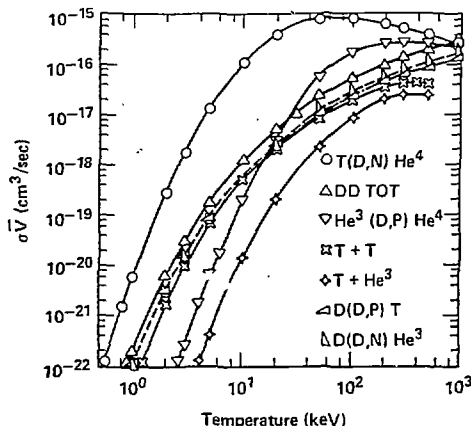


Figure 3. Thermonuclear reaction rates are strongly temperature dependent and DT is by far the easiest fuel to ignite.

nearly constant and we have approximately:

$$\phi = \frac{\rho r}{\rho r + 6 \text{ g/cm}^2} \sim \left( \frac{N_t}{N_t + (3 \text{ to } 5) \times 10^{15} \text{ sec/cm}^3} \right)$$

where we have related number density  $N_t$  to the mass density  $\rho$  by:

$$N_t = 6.02 \times 10^{23} \frac{Z}{A} \rho \sim 2.4 \times 10^{23} \rho \text{ for DT}$$

The product  $\rho r$ , which is generally expressed in g/cm<sup>2</sup> is equivalent to the  $N_t$  requirement generally used for Magnetic Fusion (MFE). We need  $\rho r = 3 \text{ g/cm}^2$  for a 33% burnup. We can use this burn efficiency formula to compare the requirements of MFE with those of ICF.

Ignition occurs when energy deposition from thermonuclear burn products during one energy confinement time equals the energy required to heat the plasma to thermonuclear burn temperatures. The energy per gram required to heat the plasma is given by:

$$E_{\text{heating}} = 0.1152 \times 10^9 T(\text{J/gm}) = 2.3 \times 10^9 \text{ J/gm} @ 20 \text{ KeV with } T_e = T_i$$

The thermonuclear burn products and energy content of various thermonuclear fuels is given in Table 1. In general, only the charged particle reaction products are available to heat the fuel since most of the neutrons escape the plasma without interacting. For DT, the alpha

Table 1.

Total energy released will determine energy output but only charged particle energy is available for self ignition of ICF size capsules.

	E (MeV)	E* (MeV) (charged particle)	Energy/ gram
D + T $\rightarrow$ He <sup>4</sup> (3.52 MeV) + n(14.06 MeV)	17.58	3.52	$3.39 \times 10^{11}$
D + D $\rightarrow$ He <sup>3</sup> (0.82 MeV) + n(2.45 MeV)			
D + D $\rightarrow$ T(1.01 MeV) + p(3.03 MeV)	3.6	2.4	$8.67 \times 10^{10}$
D + He <sup>3</sup> $\rightarrow$ He <sup>4</sup> (3.67 MeV) + p(14.67 MeV)	18.34	18.34	$3.53 \times 10^{11}$
T + T $\rightarrow$ He <sup>4</sup> + n + n	11.32		$1.82 \times 10^{11}$

particle from the reaction contains about 20% of the total energy produced. If we assume that all of the alphas are deposited, then the energy per gram deposited in the fuel is given by:

$$E_{\text{thermonuclear}} = \frac{6.68 \times 10^{10} n\tau}{\alpha\text{-particle}} \text{ J/gm} @ 20 \text{ keV}$$
$$n\tau + 5 \times 10^{15}$$

Ignition occurs for  $n\tau > 1.7 \times 10^{14}$  or  $\rho r = 0.21$  and corresponds to a burn efficiency of about 3.4%. Ignition is adequate for an MFE plasma if the energy required to maintain confinement is much less than the energy to heat the plasma. This is possible, in principle, if confinement is maintained using superconducting magnets. However, ignition alone is insufficient for ICF which must overcome a factor of 10-20 in implosion efficiency and a factor of 3-20 in driver efficiency.

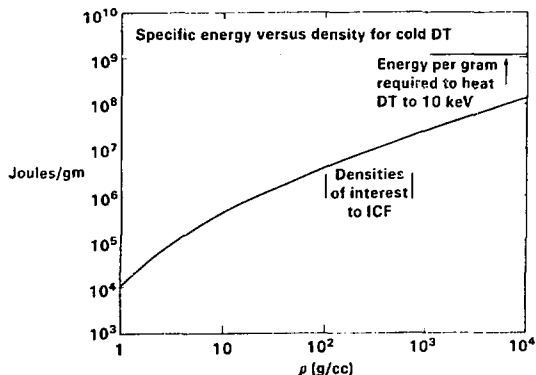
One of these factors of 10 can be recovered by increased burn efficiency. Compression of the DT fuel mass makes it feasible, in the laboratory, to achieve the  $\rho r = 3 \text{ g/cm}^2$  necessary for a burn efficiency of 1/3. For a sphere we have:

$$M = \frac{4\pi}{3} \rho r^3 = \frac{4\pi}{3} \frac{(\rho r)^3}{\rho^2}$$

Hence, the mass (and also driver energy) required for  $\rho r = 3 \text{ g/cm}^2$  scales as  $1/\rho^2$ . At normal liquid density of  $0.21 \text{ g/cm}^3$ , more than 2.5 Kg of DT is required. If this much mass were ignited, it

would have a yield of about 70 kilotons. On the other hand, at a density of 400 g/cc, a spherical shell with a thickness of  $r/2$  and radius  $r$ , would have  $\rho r = 3$  with a mass of 5 mg. This mass would have a yield of about 500 MJ and is readily contained. At 5-6 pulses per second, such targets could drive a 1 gigawatt reactor for power production. As shown in Fig. 4, if the DT remains nearly Fermi degenerate during compression, then compression is economical because the energy required is small compared to that required for ignition of the same mass of fuel.

Although compression is energetically attractive, and reduces the driver size required for efficient burn, high gain also requires hot spot ignition. For example, it takes  $5 \times 10^4$  J to compress 5 mg to 400 g/cc. But to heat that mass to 5 keV would require  $2.5 \times 10^6$  J. If the implosion had an overall efficiency of 5%, the driver size would have to be about  $5 \times 10^7$  J. This is near the upper limit of what could be considered for a laboratory driver, yet the target gain, for a burn efficiency of 1/3 would only be 10. On the other hand, if the target can be ignited from a central hot spot containing about 2% of the total mass, then the energy required to heat this mass is only about  $5 \times 10^4$  J. The total energy invested in compression and ignition would be about  $10^5$  J ( $2 \times 10^7$  J/gm), the driver size would be  $2.5 \times 10^6$  J.



- Compression reduces the mass required for a fixed burn efficiency

$$M \sim \frac{4\pi}{3} \frac{(\rho r)^3}{\rho^2}$$

- Entropy in fuel must not exceed that for  $\sim 1$  Mbar shock for peak pressures of  $\sim 100$  Mbar

Figure 4. For densities of interest to ICF, Fermi degenerate compression requires much less energy than ignition.

and the gain would be 250. Hence, for most practical applications, ICF capsules must utilize central ignition and propagation into the surrounding DT. The typical configuration of the compressed fuel at ignition is shown in Fig. 5. The hot spot  $\rho r$  must exceed the alpha particle range, shown in Fig 6 as a function of temperature, for effective self heating from 5 keV.

The energy, pulse length, and power requirements for typical ICF targets are readily estimated from target size and implosion velocity. Although a minimum average energy of  $2 \times 10^7$  J/gm of fuel is required for compression and ignition, detailed numerical calculations and experiments indicate that about twice this minimum is required for actual capsules. This corresponds to an implosion velocity of  $v = 3 \times 10^7$  cm/sec. If the overall implosion efficiency is about 5% and the fuel mass is 5 mg, then the driver energy is  $E = 4.5 \times 10^6$  J. The radius of a target with 5 mg of fuel would be about  $R = 3$  mm. The pulse length for delivery of the energy is about  $\tau = R/v = 10$  ns. The driver power is approximately  $E/\tau = 4.5 \times 10^{14}$  watts and the intensity on target is about  $4 \times 10^{14}$  W/cm<sup>2</sup>. Detailed numerical calculations of the performance of cryogenic single shell targets, as

#### DT fuel at ignition for a typical high gain capsule

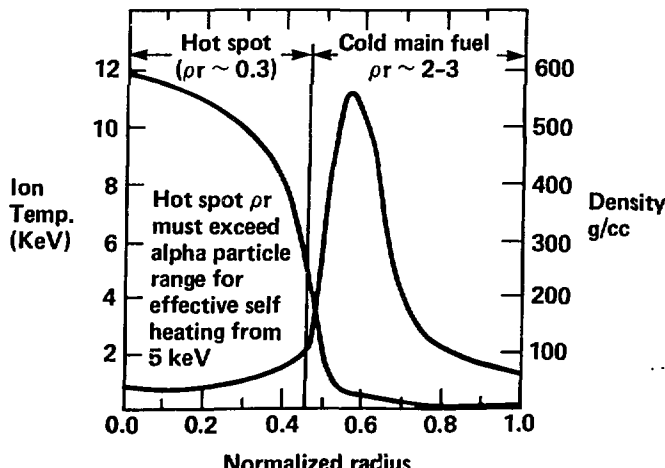


Figure 5. ICF capsules must utilize central ignition and propagation into compressed DT to achieve high gain.

shown in Fig. 7, are consistent with gains of about 100 for targets of this size.

The implosion of an ICF capsule can be described by a rocket equation:

$$V_{\text{shell}} = V_{\text{exhaust}} \ln \frac{m_0}{m_f} = \frac{P_a}{\dot{m}} \ln \frac{m_0}{m_f}$$

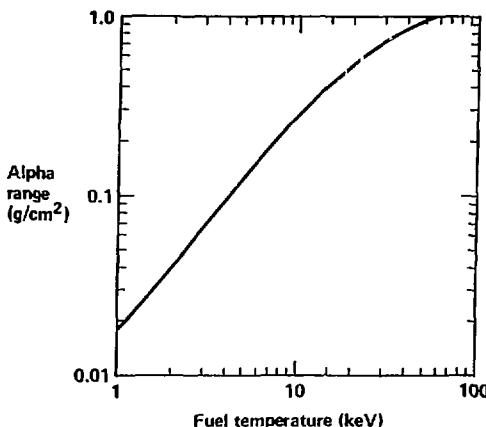


Figure 6. Efficient alpha capture requires  $\rho r > 0.3 \text{ g/cm}^2$ .

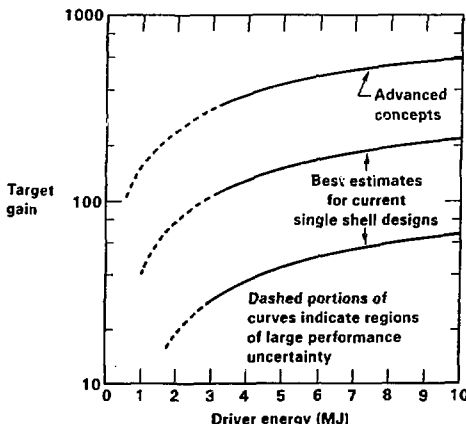


Figure 7. We expect cryogenic single shell targets to have gains in excess of 100 for multimegajoule targets.

In this equation  $P_a$  is the ablation pressure,  $\dot{m}$  is the mass ablation rate per unit area,  $m_0$  is the initial shell mass, and  $m_f$  is the fuel or payload mass. The rocket efficiency versus  $m_f/m_0$  is shown in Fig. 8 for both an ideal rocket and an ablation driven rocket. The peak efficiency of an ablation driven rocket is typically a factor of 4 or more less than that of an ideal rocket. In an ablation driven rocket, the exhaust, the target corona, is heated so that it remains nearly isothermal instead of cooling to zero temperature as assumed for the ideal rocket.

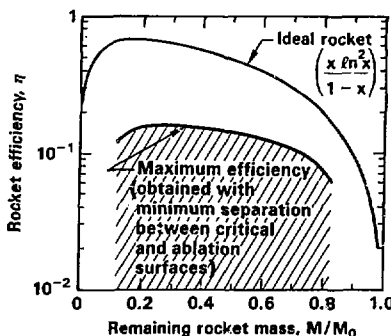
As mentioned earlier, implosion symmetry is an important issue for high convergence ratio targets. If a target with an initial radius  $R$  and average implosion velocity  $v$  has a location on its surface with velocity perturbation  $\delta v$ , then the deviation from sphericity as it implodes is given by:

$$\delta R = \delta v t \sim \delta v \frac{R}{v}$$

If we require that this deviation be less than  $1/2 r$ , the final compressed radius, we have:

$$\frac{\delta v}{v} < \frac{1}{2} \frac{r}{R}$$

Since  $R/r = 30-40$  is typical, we require implosion velocities which are uniform to about 1% and energy fluxes to the capsule which are uniform to about 2%. Figure 9 shows the results of detailed numerical



— Maximum efficiency is lower than classical rocket because exhaust is heated

Figure 8. Subsonic ablation follows an isothermal rocket equation.

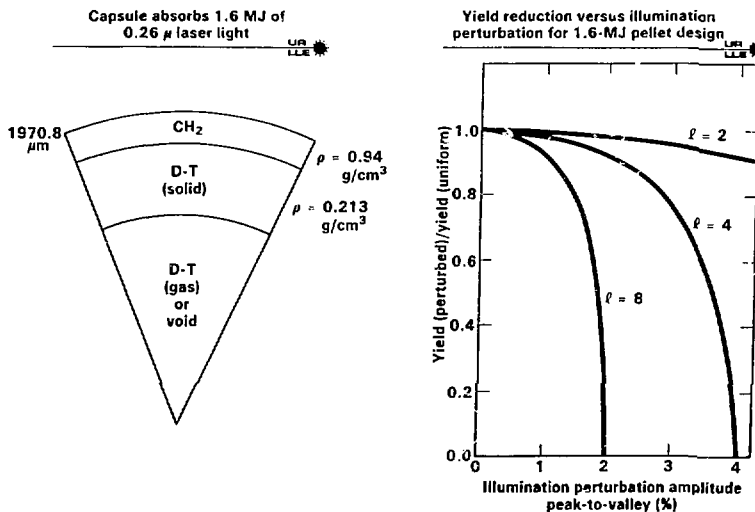


Figure 9. Near optimal performance of high gain capsules requires fluxes that are uniform to about one percent.

calculations carried out at the University of Rochester for a capsule which absorbs 1.6 MJ of 0.26 micron laser light. Plotted in Fig. 9 is the calculated yield in the presence of an intensity perturbation divided by the calculated yield with uniform intensity. This ratio is plotted for the perturbation in three different spherical harmonic mode numbers  $\ell = 2, 4$ , and  $8$ .

In general, ICF capsules rely on either electron conduction (direct drive) or x-rays (indirect drive) to drive an implosion.

In direct drive, the laser beams (or charged particle beams) are aimed directly at a target. The laser energy is transferred to electrons via inverse bremsstrahlung or a variety of plasma collective processes. This absorption occurs at a density equal to or less than the plasma critical density

$$n_c = \frac{10^{21}}{\lambda^2}$$

where  $\lambda$  is the laser wavelength in microns. Electron conduction must transport the energy to the ablation front which typically has an electron density of about  $10^{24}/\text{cc}$ . Uniformity of the flux must be obtained by direct overlap of a large number of very uniform beams, or by lateral electron conduction smoothing. In steady state, a

perturbation in intensity  $\delta I_0$  will be smoothed by electron conduction approximately according to the formula:

$$\delta I = \delta I_0 \exp\left(-\frac{2\pi\delta r}{L}\right)$$

where  $L$  is the spatial scale of the perturbation and  $\delta r$  is the separation between the absorption surface and the ablation surface. In order to minimize various plasma collective effects and to maximize hydrodynamic efficiency, almost all current work on direct drive utilizes laser wavelengths which are less than 0.5 microns. For such short laser wavelengths,  $\delta r$  is only a few microns and conduction smoothing is ineffective for all but the shortest scale perturbations. Hence, uniformity must be achieved by overlapping a sufficiently large number of high quality beams. Figure 10 shows the expected uniformity calculated by the University of Rochester with various numbers of laser beams as a function of the focus ratio. The focus ratio is the ratio of the beam radius to the initial target radius. To keep the total solid angle subtended by the beams fixed in these calculations, the  $f$ -number of the beams was increased as the beam number increased. Adequate uniformity must be obtained over a focus ratio of about a factor of 2 because the target radius decreases about a factor of two during the time that the laser beam irradiates the target. These

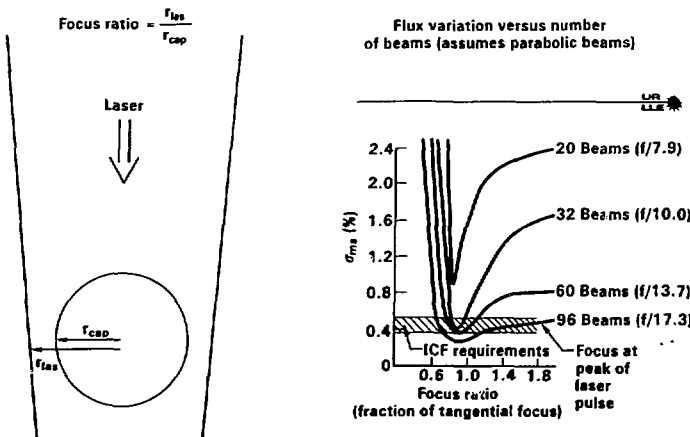


Figure 10. A large number of beams is required to obtain adequate symmetry for direct drive targets in the absence of conduction smoothing.

calculations assume no pointing errors, perfect beam balance, and smooth beams. As seen in Fig. 10, approximately 100 beams is required for adequate uniformity. Developing the technology required to achieve uniformity with short wavelength lasers has been a major focus of research on direct drive for the past five years. Although no current laser system designed for direct drive implosions can deliver the required uniformity, much progress has been achieved in developing individual beams which have the required smoothness.

In the x-ray or indirect drive approach to ICF, the laser beams are first absorbed on a high-Z enclosure, a hohlraum, which surrounds the capsule. A significant fraction of this absorbed energy is converted to x-rays which then drive the capsule implosion. This two step process results in a decoupling of the absorption and smoothing processes and greatly relaxes the beam quality requirements. Experiments done on the Nova laser at Lawrence Livermore National Laboratory (LLNL) have demonstrated that fluxes uniform to a few percent can be achieved inside hohlraums. This uniformity was demonstrated by imaging the compressed fuel region of an x-ray driven implosion. The experiment utilized a 100 psec framing camera, shown schematically in Fig. 11, to image x-rays emitted by an Argon tracer in the fuel. The images shown in Fig. 12 were obtained from a pair of experiments. The left hand image was obtained from a hohlraum which

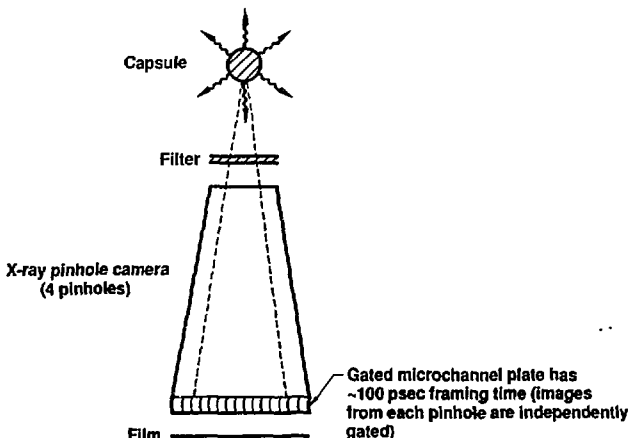


Figure 11. X-ray framing cameras have played a major role in recent demonstrations of highly uniform implosions.

- Target symmetry is measured with a 100 psec x-ray framing camera

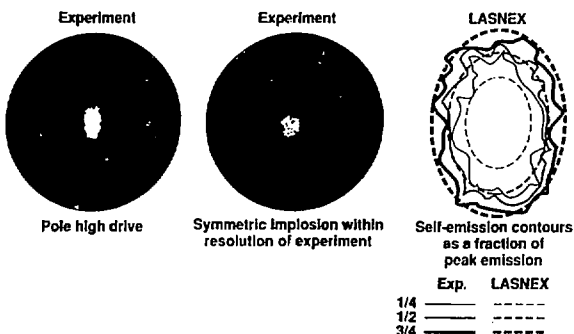


Figure 12. Control of drive symmetry and high uniformity has been obtained with hohlraum targets.

was deliberately designed to have an asymmetric drive. The right hand image was obtained from an optimized hohlraum and is round to within the resolution of the instrument. A comparison of the asymmetric image to a LASNEX numerical simulation shows that we are able to accurately calculate both the shape and size of the imploded fuel region. This ability to accurately control symmetry is one of the major reasons that radiation drive is the primary approach being pursued by the U.S. ICF Program.

For radiation drive to achieve high gain, it is necessary to convert a large fraction of the driver energy into x-rays. Both lasers and ion beams can achieve high x-ray conversion efficiency, but they have opposite intensity scaling as shown in Fig. 13. For intensities of interest, the laser x-ray conversion efficiency increases as the laser wavelength decreases and as the intensity decreases. As described earlier, the laser absorption occurs in material at or below the critical density. At high temperature or long laser wavelength, this absorption generally produces temperatures which are too high in a density which is too low for optimal reradiation of the absorbed energy as x-rays. Electron conduction must transport the absorbed energy to a higher density and lower temperature region where most of the x-rays are produced. As the intensity drops, or as the laser wavelength

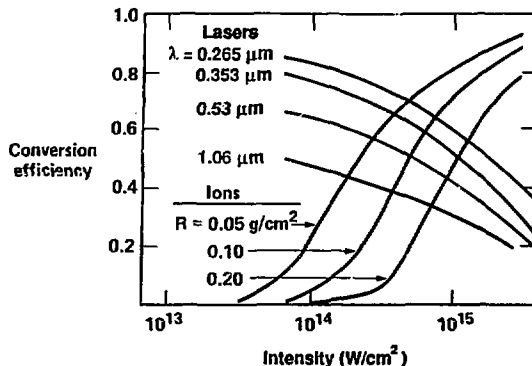


Figure 13. Both lasers and ion beams can achieve high x-ray conversion efficiency but have opposite intensity scaling.

decreases, the absorption produces more nearly optimal conditions so that losses incurred in the transport process are less and conversion efficiency is higher. The minimum useful intensity on target is about  $10^{14}$  W/cm<sup>2</sup>. Below that intensity, conditions produced in the target are no longer optimal for a capsule implosion.

For ions, the conversion process is very different. Ion beams are generally absorbed in a low-Z material which heats up and then radiates like a black body. The energy balance equation for an ion beam can be written as:

$$I = R \frac{d\epsilon}{dt} + \frac{dK}{dt} + \sigma T^4$$

where R is the ion range in g/cm<sup>2</sup>,  $\epsilon$  is the specific energy of the absorber, and K is the kinetic energy of expansion of the absorber. The heat capacity term, which is proportional to the temperature T, is the dominant term at low temperature. At high temperature, the radiative term dominates. The kinetic energy term can generally be made small by appropriate choice of absorber material. If the intensity is too low, the absorber material never heats up sufficiently to become an efficient radiator before the pulse ends. At high intensity, the absorber heats up quickly, and then radiates very efficiently. The intensity required for efficient conversion increases

as the range increases since the longer range results in a higher heat capacity of the absorber and a longer time before radiation becomes efficient. Figures 14a and b show the energy balance at two intensities for 10 ns pulses and a range of  $0.1 \text{ g/cm}^2$ , a range comparable to that of 10 GeV lead ions.

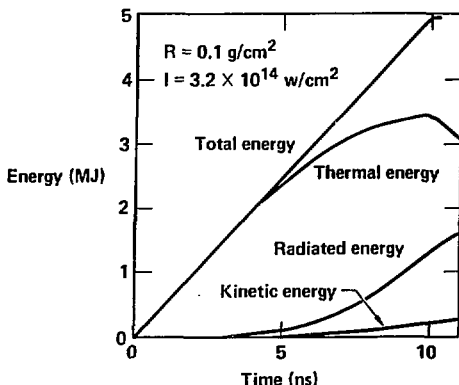


Figure 14a. Low intensity gives low radiation temperature and high thermal losses.

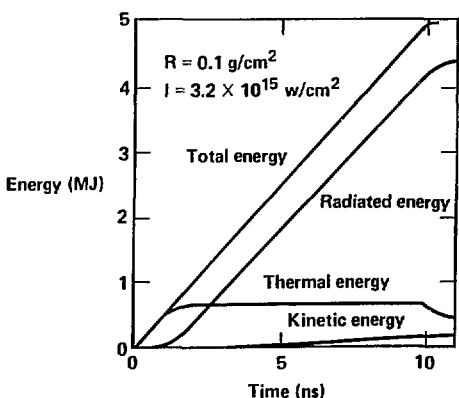


Figure 14b. High conversion efficiency requires low kinetic and thermal energy losses.

To efficiently compress DT to several hundred grams per cubic centimeter with a laser, the compression must be near Fermi degenerate. This means that the pressure in the fuel at a given density must be near the Fermi pressure. To achieve this, the entropy generated in the fuel must be limited to that generated by about a 1 Mbar shock. Since the peak pressures must be about 100 Mbar, the pressure generated in the shell must be increased from 1 Mbar to 100 Mbar in such a way that little additional entropy is generated. If we imagine that the pressure is increased in incremental steps, then little entropy is generated if the pressure change from one step to another is less than about a factor of 4. This result can be obtained from the Hugoniot relations. To increase the pressure from 1 Mbar to 100 Mbar requires four or more steps. Various types of pulse shapes which will accomplish this objective are shown in Fig. 15. The timing of the various shocks must be such that all the shocks coalesce near the inside surface of the main fuel. This insures that all of the main fuel sees a series of pressure pulses which differ by no more than a factor of 4 in pressure. This timing also insures that the central gas region sees one large shock which puts it on a very high adiabat. A high adiabat is necessary for the formation of the ignition hot spot.

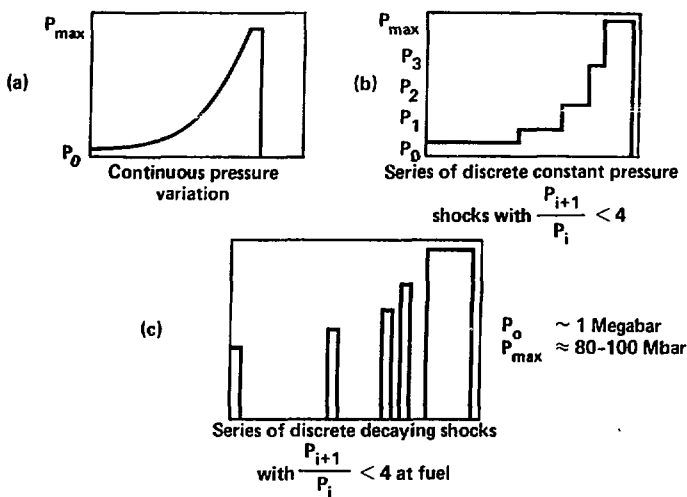


Figure 15. A variety of equivalent pulse shapes can provide the required temporal history of the pressure on the fuel.

A final topic of critical importance to the operation of ICF capsules is hydrodynamic instability during the implosion process. The dense central region of the capsule is imploded by the low density, high temperature corona produced by ablation. This is a situation similar to the classic Rayleigh-Taylor (RT) instability which occurs in a gravitational field when a low density fluid  $\rho_1$  supports a high density fluid  $\rho_2$ . The growth rate of these RT like modes can be written as:

$$\gamma = \epsilon \sqrt{\frac{ka(\rho_2 - \rho_1)}{\rho_2 + \rho_1}}$$

$a$  = acceleration  
 $k$  = wave number of the perturbation  
 $\frac{\rho_2 - \rho_1}{\rho_2 + \rho_1}$  = Atwood number

where  $\epsilon < 1$  because of density gradient and ablation effects. If the shell acceleration is constant and the shell is accelerated a distance  $R/2$ , then the number of e-foldings of growth for a surface perturbation, when  $\rho_1 \ll \rho_2$ , is given by:

$$n = \gamma dt = \epsilon \sqrt{KR}$$

RT modes are surface modes which saturate when their amplitude is comparable to a wavelength. Hence, short wavelength modes will saturate before they reach significant size. Very long wavelength modes on the other hand grow very slowly and do not reach large amplitude before the end of the implosion. Hence, the most critical modes are those with a wavelength comparable to the shell thickness. If we use this wavelength in the formula for the number of e-folding, we have:

$$n \sim \epsilon \sqrt{2\pi R/\Delta R}$$

This shows that the growth of RT modes is primarily a function of the shell aspect ratio. If the maximum acceptable amplification is a factor of 1000, then the aspect ratio must be limited to:

$$R/\Delta R < 7.6/\epsilon^2$$

For  $\epsilon \sim 1/2$ , we expect that  $R/\Delta R = 30$  is about the limit for acceptable aspect ratios. IFAR is related to the implosion pressure. A simple model which shows this is the following. We have

$$R = 1/2 at^2 \quad (a = \text{constant})$$

$$V = at = \sqrt{2Ra} = \sqrt{2 \frac{P}{\rho} \frac{R}{\Delta R}}$$

$$\text{or } \frac{R}{\Delta R} = \frac{1/2 \rho v^2}{P}$$

For Fermi degenerate compression we have:

$$P(\text{Mbar}) = 2\rho^{5/3} \text{ g/cc}$$

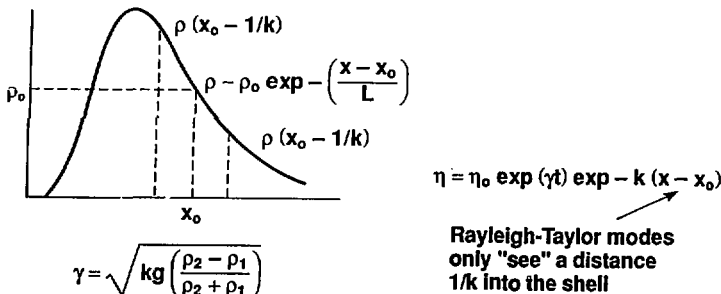
$$\frac{R}{\Delta R} = \frac{v^2 (\text{cm}/\mu\text{sec})}{3\rho^{0.4} (\text{Mbar})}$$

for  $P = 100 \text{ Mbar}$  and  $v = 24 \text{ cm}/\mu\text{sec}$ , we have:

$$\frac{R}{\Delta R} = 30$$

If the growth rates of the RT instability were not reduced from its classical value, ICF would not be achievable with pressures which can be obtained in the laboratory. Two effects reduce the growth rate from its classical value: density gradients and ablation.

The effects of a density gradient are shown in Fig. 16. The growth rate of RT modes depends on the magnitude of the density jump across an interface between two materials. Since the RT modes are surface modes,



$$\frac{\rho_2 - \rho_1}{\rho_2 + \rho_1} \sim \frac{\rho(x_0 + 1/k) - \rho(x_0 - 1/k)}{\rho(x_0 + 1/k) + \rho(x_0 - 1/k)} \Rightarrow$$

$$\frac{1}{kL} \text{ for } kL \gg 1$$

$$1 \text{ for } kL \ll 1$$

$$\gamma \sim \sqrt{\frac{kg}{1 + kL}} g$$

Figure 16. Density gradients reduce the effective density jump at the ablation surface.

the perturbation only "sees" density differences which occur within a distance  $1/k$  from the surface. If there is a density gradient in the material instead of a sharp density discontinuity, the gradient has the effect of reducing the density jump at the interface as indicated in Fig. 16. The growth rate in the presence of a density gradient becomes:

$$\gamma = \sqrt{\frac{ka}{1+KL}}$$

where  $L$ , as defined in Fig. 16 is the density gradient scale length. The density gradient at the ablation front is affected by photon and electron preheat and can be optimized to be about half the shell thickness.

The second effect which reduces the growth rate at the ablation surface is the ablation process itself. In the absence of ablation, the instability is centered about the original discontinuity in density and its amplitude decreases exponentially in amplitude away from this surface. Ablation moves the location of the density jump into this region of lower amplitude, effectively giving a lower growth rate at the ablation surface. This effect is shown in Fig. 17 and results in a growth rate given by:

$$\gamma = \gamma_0 - kV_a$$

where  $V_a = \frac{\dot{m}}{\rho}$  is the velocity at which the ablation front moves into the shell.

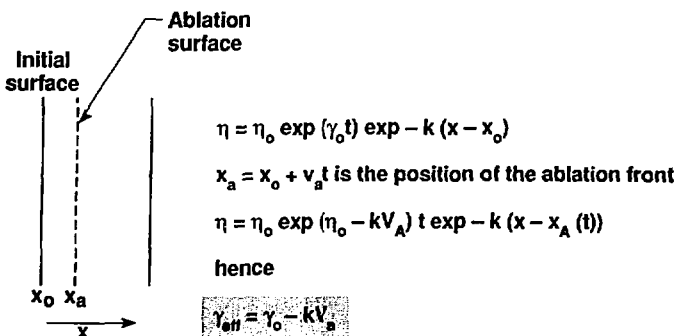


Figure 17. Ablation advects perturbed material from the surface leaving a smoother surface and effectively lower growth rate.

If these two effects are optimized and taken together, they result in a major reduction in the growth of RT modes as shown in Fig. 18 for  $R/\Delta R = 25$ . Above a cutoff wavelength, the modes are no longer unstable at all. If we integrate the dispersion relation with density gradients and ablation included, under the assumption of constant acceleration for a distance  $R/2$  as before, we get the number of e-folding plotted in Fig. 19 for  $R/\Delta R = 25$  and  $R/\Delta R = 225$ . It is clear that even with these stabilizing effects, very high aspect ratio shells will have excessive growth. Modest aspect ratio shells with  $R/\Delta R \sim 25$ , however, have only a few e-foldings of growth during acceleration.

This single mode analysis is indicative of the effects of RT modes on an ICF capsule. In a real capsule, a whole spectrum of modes is growing at once. Many of these modes can reach nonlinear saturation. Mode-mode coupling can result in saturated modes feeding modes which have not yet saturated. Theories which incorporate all of these effects are still being developed. But current conclusions from the best analysis and data available indicates that shells with  $R/\Delta R = 30$  can be imploded successfully. In general, radiation driven implosions can be designed to have lower RT growth rates than direct

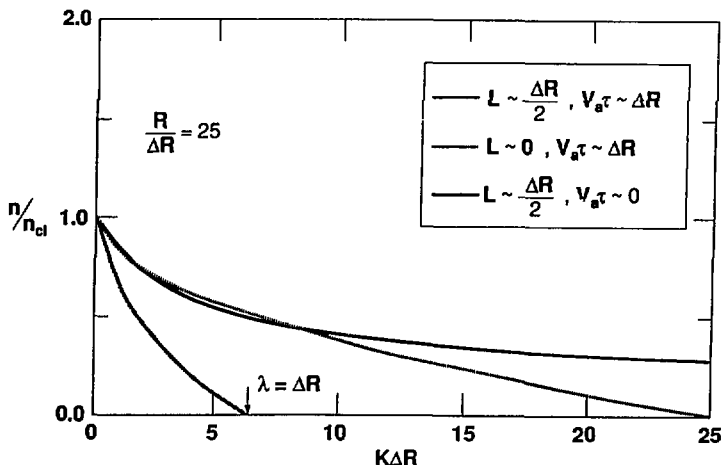


Figure 18. If ablation and density gradients are optimized, Rayleigh-Taylor instabilities can be strongly stabilized.

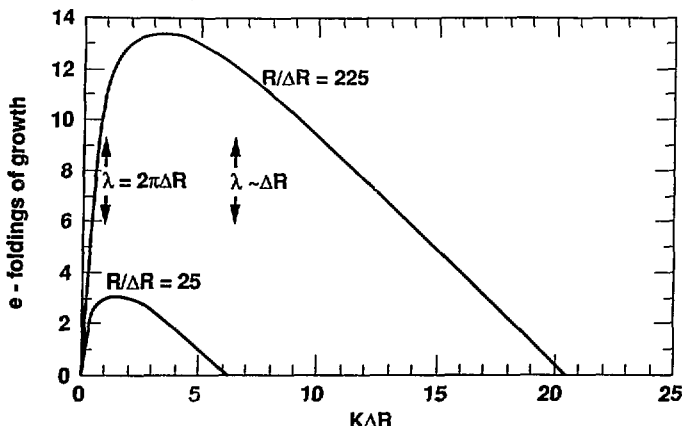


Figure 19. When ablation and density gradient effects are optimized, implosion of moderate aspect ratio shells results in acceptable growth of perturbations.

drive targets. This is the second major reason that radiation drive has played the leading role in the U.S. ICF Program.

In summary, ICF targets must achieve densities of several hundred grams per cubic centimeter and utilize hot spot ignition to achieve high gain. For this to be possible, ICF capsules must:

- 1) Reach implosion velocities of about  $3 \times 10^7$  cm/sec
- 2) Have implosion velocities uniform to about 1%
- 3) Utilize pulse shaping sufficient to maintain a near Fermi pressure limited compression of the fuel
- 4) Control hydrodynamic instabilities sufficiently to allow  $R/\Delta R = 30$ .